

Effect of calcination and chromium doping on the structural characteristics of titanate nanotubes

A. H. Shahbazi Kootenaeei, S. Maghsoodi

Department of Chemical Engineering, Mahshahr Branch, Islamic Azad University, Mahshahr, Iran.

Received June 26, 2015; Revised September 10, 2015

Titanate nanotubes were synthesized by alkaline hydrothermal method using TiO₂ P25 at 140°C. In the present study the effects of calcination and chromium doping was investigated. At various chromium concentrations some phase changes occurred. The BET specific surface area altered from 404 m²g⁻¹ to lesser values by chromium loading augmentation. Calcination process accelerated the phase transformation from hydrogen titanate to anatase polymorph of TiO₂ along with specific surface area deterioration. In the range of the studied parameters, the emergence of rutile phase was not confirmed. Calcination of 1 wt% and 2 wt% chromium doped titanate sample induced the chromium oxide phase development. Calcination process brought about nanotubular structure deterioration along with nanoparticles evolution.

Keywords: Titanate nanotubes; Chromium; Doping; Anatase; Calcination.

INTRODUCTION

Kasuga et al. [1] recently announced the synthesis of TiO₂-derived nanotubular structures by hydrothermal treatment of titania powder in a concentrated NaOH aqueous solution. The aforementioned method is a template-free one producing elongated nanotubes with diameters of ca. 10 nm. These rather novel nanostructures are characterized by a high specific surface area [2].

Affecting from many parameters such as synthesis and calcination temperatures, dopants, and etc., the abovementioned hydrothermal method offers a simple, cost-effective, and environmentally friendly technology with the potential of high-yield titanate nanotube production [3-6].

These novel structures can be modified by grafting [7], ion-exchange [8], calcination, and treatment with chemical agents [9, 2].

Metal ion incorporation into titanate nanotubes will definitely alter the properties, however, as a consequence of metal ion insertion, the structure of nanotubes can be greatly affected as well.

Wang et al. [10] synthesized titanate nanotubes doped with magnetic ions (Fe, Ni, and Mn) that were synthesized by hydrothermal method as the ions were added to the nanostructure during the formation process of nanotubes. The as-prepared nanotubes transformed into the anatase polymorph of titania when the calcined temperature surpassed

350K, and further transformed into the mixture of anatase and rutile phases in consort with temperature rise.

Kulish et al. [11] found that the structure of (Fe, Mn, Zn, Cd, and Ni) doped nanotubes is analogous to Na₂Ti₂O₄(OH)₂ structure. Also, they suggested that the structure of Cd doped nanotubes may be a mixture of anatase and rutile polymorph of titania. Their results led to the conclusion that the examined metals did not form a solid solution of metal with titania. Besides, they asserted that the ions adsorption occurred on external and internal surfaces of the nanotubes.

In this contribution, calcined/uncalcined titanate nanotubes with/ without doping with chromium were examined for phase transformation behavior as well as specific surface area alteration using XRD and BET techniques. A morphology study was performed on the calcined chromium-containing sample by HRTEM technique in order to probe the morphology change.

EXPERIMENTAL

Preparation of Cr doped titanate nanotubes

For preparation of titanate nanotubes, 1.7 g of TiO₂ powder (Degussa P25) along with various amounts of chromium nitrate was added to aqueous solution of NaOH (10M) with constant stirring for 30 min. A Teflon-lined stainless steel autoclave with a capacity of 180 mL was filled with the resulting mixture up to about 80% of its total volume. The autoclave was sealed and heated at 140°C for 24 h. After the reaction was completed,

To whom all correspondence should be sent:
E-mail: kootena@gmail.com

the autoclave was allowed to cool to room temperature naturally. Then, the resulting material subjected to centrifugation and washing with a diluted 0.1M HNO₃ acid solution. The washing process continued until the pH of the rinsing solution reached about 1. The precipitates then washed with deionized water until the pH of washing solution achieved about 7. The acid-treated sample was oven-dried at 110°C overnight.

In TNT-x (x=0.2, 0.5, 1, and 2), "x" represents weight percent of chromium oxide in Final uncalcined samples. In the sample names, "C" represent calcination of samples at 500°C.

All chemical materials were purchased from Merck Company.

Material Characterization

X-ray diffraction (XRD) patterns of the samples were obtained with a Philips PW1800 diffractometer using Cu K α radiation. The intensities were determined over an angular range of $5^\circ < 2\theta < 70^\circ$ for all the prepared samples with a step-size $\Delta(2\theta)$ of 0.03° and a count time of 2 seconds per step. The diffraction spectra have been indexed by comparison with the JCPDS files (joint committee on powder diffraction standards).

Sample morphology was investigated by "JEOL" JEM-2100 (200 kV) high resolution transmission electron microscope (HRTEM). For HRTEM measurements the sample was grounded, suspended in isopropanol at room temperature and dispersed by ultrasonic agitation. Then, an aliquot of the prepared solution was dropped on a 3mm diameter lacey carbon copper grid.

The specific surface areas (S_{BET}) of the samples were determined at the liquid nitrogen (N₂) temperature from the adsorption and desorption isotherms of nitrogen by a Quantachrome CHEMBET-3000 apparatus using single-point method. Prior to BET surface area measurement samples were degassed by flow of nitrogen at 200°C for 2h.

RESULT AND DISCUSSION

HRTEM analysis

The HRTEM analysis performed on the CTNT-2 for the sake of investigating possible morphology alteration stemmed from chromium addition (Fig. 1). As can be noted, the nanotube morphology along with other nanostructures such as nanorod and nanoparticles is observed. Nanowire are estimated possessing diameters about 20 nm. Calcination exerted detrimental effects on nanotubular structure of pristine chromium doped

titanate nanotubes. As will be noted in section 3.2, doping with chromium led to specific area loss. Therefore, phase transformation from nanotubular structure into other morphologies such as nanoparticles as well as chromium oxide development (see next section) may be responsible for this observation. It has been reported that metal incorporation in nanotubular titanates altered the phase transformation in the acceleration or deceleration of the tubular phase deterioration can be observed [2, 12-14].

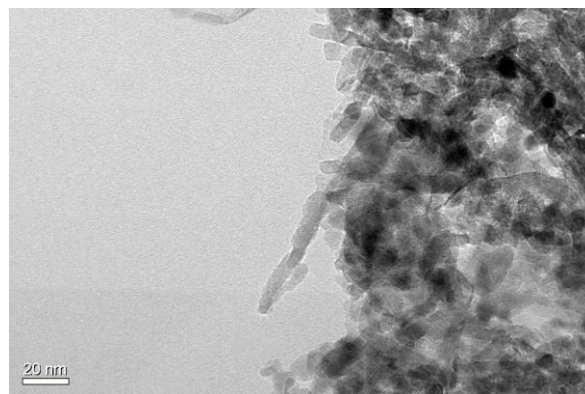


Fig. 1. HRTEM micrograph of CTNT-2.

XRD and BET analysis

The X-ray diffraction patterns acquired from uncalcined samples of undoped titanate nanotubes and chromium doped titanate nanotubes are shown in Fig. 2. The structure of undoped pristine nanostructures proposed to be H₂Ti₂O₅·H₂O in our previous work [2].

According to the XRD analysis, TNT-0.2 (Fig. 2b) differs slightly as compared to pristine undoped titanate nanotube (TNT) (Fig 2a). Hence, 0.2 wt% chromium loading hardly affected the crystalline structure of titanate nanotube. In the other hand, BET specific surface area dropped about 10% for this sample. This may be ascribable to the slight morphology change of TNT. The characteristic peak intensities of titanate nanotubes lowered for TNT-0.5 (Fig. 2c) as compared to the ones for TNT, which is ascribable to the crystal growth and emergence of new phase. It is noteworthy to claim that no characteristic peak assignable to the crystalline chromium oxide was observed. Chromium species may occurred in undetectable sizes beyond the capacity of XRD apparatus [15, 16]. The corresponding XRD patterns of TNT-1 is depicted in Fig. 2d. A noticeable shift in the peak located originally at $2\theta=10^\circ$ for pristine undoped titanate nanotube was observed, for TNT-1 sample. The alteration in the roll distances is reported to be responsible for this observation. Besides, BET

specific surface area decline was also reported to be accompanied with this phenomena [10, 11].

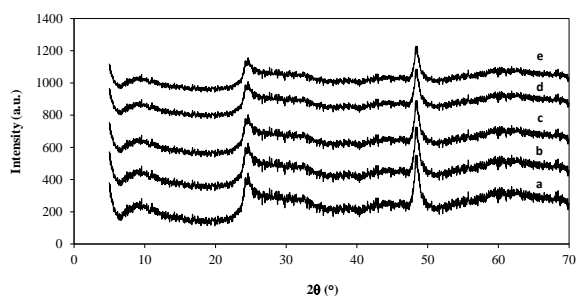


Fig. 2. XRD patterns of (a) uncalcined acid-treated titanate nanotubes [2], (b) TNT-0.2, (c) TNT-0.5, (d) TNT-1, and (e) TNT-2.

No characteristic peaks of the typical polymorph of titanate dioxide naming anatase, rutile and/or brookite were distinguishable.

It has been reported that some titanate phase may convert to titanium oxide with anatase phase. Generally, the greater the metal oxide doping, the higher the possibility of metal oxide crystalline phase development [15, 17]. Like the other analyzed samples, we could not find the characteristic peaks associable to the presence of the crystalline phase of chromium oxide in the TNT-2 (Fig. 2d) with the highest metal oxide loading. No characteristic peaks of anatase and/or other polymorphs of TiO_2 was present in this sample.

XRD analysis was performed on the CTNT-x samples calcined at 500°C (Fig. 3). As can be noted from Table 1, BET specific surface area of pristine undoped titanate nanotube lowered from $404 \text{ m}^2\text{g}^{-1}$ (TNT) to $186 \text{ m}^2\text{g}^{-1}$ (CTNT). Similar reports support this observation. Gao et al. [18] investigated the phase transformations of titanate nanotubes by in situ XRD. In their report, dehydration and recrystallization claimed to be the main causes of anatase phase emergence in calcination temperatures above 300°C which is accompanied by specific area loss. Water molecules along with the protons present loosely between the layer that are mobile and exchangeable by external ions. Poudel et al. [19] reported that titanate nanotubes are prone to transform into anatase phase of titanium oxide through calcination in air at rather

elevated temperatures. This process is a function of calcination temperature, impurities (intentional or unintentional), atmosphere, and etc. [20, 21]. However, this is a controversial research topic and the issues are under debates. As can be seen in the acquired XRD patterns shown in Fig. 3, the phase transformation from hydrogen titanate to anatase is obvious. In all of the calcined samples, XRD patterns hints that rutile phase may not coexist with anatase phase in the heat treated chromium doped titanate nanotubes.

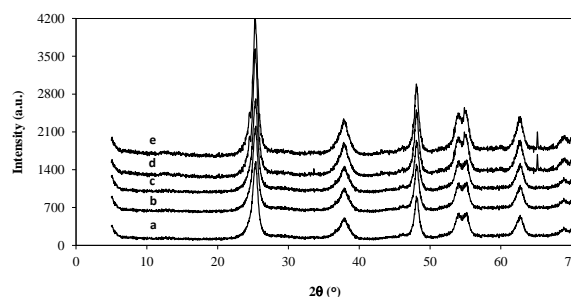


Fig. 3. XRD patterns of (a) calcined titanate nanotubes, (b) CTNT-0.2, (c) CTNT-0.5, (d) CTNT-1, and (e) CTNT-2.

BET specific surface area of CTNT-0.2 dropped to $164 \text{ m}^2\text{g}^{-1}$ due to calcination. We could not find any peaks that can be ascribable to the presence of chromium oxide phase. This may be due to the fact that XRD apparatus has limited detection capacity which for lower than a certain particle sizes no characteristic peak of the crystalline phase is demonstrated in the obtained patterns. BET specific surface area of CTNT-0.5 lowered to $150 \text{ m}^2\text{g}^{-1}$. As can be noted, increasing the chromium content led to surface area loss. The XRD patterns of CTNT-1 is shown in Fig. 3d. This sample possess a specific surface area of $98 \text{ m}^2\text{g}^{-1}$. The characteristic peaks ascribable to the presence of chromium oxide phase can be observed clearly. The characteristic peaks of this phase demonstrate at $2\theta=24.49^\circ$, 33.59° , 36.19° , 41.47° , 50.21° , 63.44° , and 65.10° (JCPDS 38-1479). The specific surface area was measured to be $66 \text{ m}^2\text{g}^{-1}$. The characteristic peaks of chromium oxide phase were measured with higher intensity that may be due to the superior population of the phase with large particles.

Table 1. BET specific surface area of the synthesized samples.

Sample	BET specific surface area m^2g^{-1}	Sample	BET specific surface area m^2g^{-1}
P25	52	CTNT	186
TNT	404	CTNT-0.2	164
TNT-0.2	362	CTNT-0.5	150
TNT-0.5	328	CTNT-1	98
TNT-1	203	CTNT-2	66
TNT-2	157		

CONCLUSION

The phase change behaviors of acid-washed titanate nanotube samples were examined by varying the chromium content as well as calcining in air. The higher the chromium loading was the lower the BET specific surface area. Also, calcination in 500°C caused a surface area loss along with the apparent new phase development for higher chromium containing samples. Chromium oxide was detected at loadings higher than 1 wt.%. The calcined samples morphology transformed from elongated nanotubular structure to truncated tubes as well as nanoparticles. No indication revealing the occurrence of rutile phase was noticed after calcination for all chromium concentrations.

Acknowledgements: Financial support for research project granted by Islamic Azad University of Mahshahr is highly appreciated.

REFERENCES

1. T. Kasuga, M. Hiramatsu, A. Hoson, T. Sekino, K. Niihara, *Langmuir*, **14**, 3160 (1998).
2. A.H. Shahbazi Kootenaeei, J. Towfighi, A. Khodadadi, Y. Mortazavi, *Appl. Surface Sci.*, **298**, 26 (2014).
3. A. Oszko, G. Potari, A. Erdo'helyi, A. Kukovecz, Z. Konya, I. Kiricsi, J. Kiss, *Vacuum*, **85**, 1114 (2011).
4. A. Kukovecz, G. Potari, A. Oszko, Z. Konya, A. Erdo'helyi, J. Kiss, *Surface Sci.*, **605**, 1048 (2011).
5. G. Potari, D. Madarasz, L. Nagy, B. Laszlo, A. Sapi, A. Oszko, A. Kukovecz, A. Erdo'helyi, Z. Konya, and J. Kiss, *Langmuir*, **29**, 3061 (2013).
6. J. Liu, Y. Fu, Q. Sun, J. Shen, *Micropor. Mesopor. Mater.*, **116**, 614 (2008).
7. L. Wang, W. Liu, T. Wang, J. Ni, *Chem. Eng. J.*, **225**, 153 (2013).
8. T. Kasuga, *Thin Solid Films*, **496**, 141 (2006).
9. R. Doong, C. Tsai, C. Liao, *Separ. Purif. Technol.*, **91**, 81 (2012).
10. M. Wang, G. Song, J. Li, L. Miao, B. Zhang, *J. Univ. Sci. Technol. Beijing, Mineral, Metallurgy, Material*, **15**, 644 (2008).
11. M.R. Kulish, V.L. Struzhko, V.P. Bryksa, A.V. Murashko, V.G. Il'in, *Semicond. Physics, Quantum Electronics & Optoelectronics*, **14**, 21 (2011).
12. K. Takashi, S. Keijiro, O. Takamasa, Yamasaki Yuki, N. Atsushi, *Mater. Trans.*, **50**, 1054 (2009).
13. J.S. Jang, D.H. Kim, S.H. Choi, J.W. Jang, H.G. Kim, J.S. Lee, *Int. J. Hydrogen Energy*, **37**, 11081 (2012).
14. A. Rónavári, B. Buchholcz, Á. Kukovecz, Z. Kónya, *J. Molec. Struct.*, **1044**, 104 (2013).
15. A.A. Lemonidou, L. Nalbandian, I.A. Vasalos, *Catalysis Today*, **61**, 333 (2000).
16. V.L. Volkov, E.I. Andreikov, G.S. Zakharova, V.Y. Gavrilov, V.V. Kaichev, V.I. Bukhtiyarov, *Kinetics and Catalysis*, **49**, 446 (2008).
17. B. Grzybowska-Swierkosz, *Appl. Catalysis A: General*, **157**, 263 (1997).
18. T. Gao, H. Fjeld, H. Fjellvåg, T. Norby, P. Norby, *Energy & Environ. Sci.*, **2**, 517 (2009).
19. B. Poudel, W.Z. Wang, C. Dames, J.Y. Huang, S. Kunwar, D.Z. Wang, D. Banerjee, G. Chen, Z.F. Ren, *Nanotechnology*, **16**, 1935 (2005).
20. R. Yoshida, Y. Suzuki, S. Yoshikawa, *Mater. Chem. Physics*, **91**, 409 (2005).
21. C.C. Tsai, H. Teng, *Chem. Mater.*, **16**, 4352 (2004).